uc3m | Universidad Carlos III de Madrid

Master Degree in Physics of Complex Systems
2021-2022

Master Thesis

Coevolution of individual perception and cooperative behavior in the Norm Compliance Dilemma

---

Author: Sara Ghivarello

Supervisor: Alberto Antonioni
Co-supervisor: Luca Dall'Asta

Madrid, 25/06/2022

Politecnico di Torino

SORBONNE UNIVERSITÉ

complex systems

ABSTRACT

Mathematical epidemiology has, now more than ever, attracted great attention in the scientific community. However, little exploration has been done in the direction of modelling human behavioural response when facing an epidemic outbreak. In this context, individuals may employ containment measures to prevent the disease spreading, i.e. providing a benefit to the entire population, at a cost that is heterogeneously perceived by each individual. In our work we study the coevolution of cooperative behaviour and individual perception through the lens of evolutionary game theory, considering the adoption of a disease containment measure as a cooperative act. We introduce this game-theoretical framework as the "Norm Compliance Dilemma", where the evolution of agents' behaviors depends on their distinct, time-evolving perceptions. Starting from a simplified model of a well-mixed infinite population having homogeneous perceptions, we studied and analytically solved a system of ordinary differential equations to predict the game equilibria. Subsequently, we compared the theoretical results with those obtained in finite populations having heterogeneous individual perceptions and organised in network structures. We show that the disease prevalence promotes cooperation, finding that this result is qualitatively confirmed regardless of the spatial arrangement of individuals or the heterogeneity of their perception. On the other hand, networked structures may hinder and slow down the evolution of cooperation with respect to well-mixed populations. Our model offers an alternative and general methodology to study heterogeneous coevolving perceptions which can be applied to different types of epidemic spreading and norm compliance scenarios.

CONTENTS

1. INTRODUCTION 1
2. METHODS 3
2.1. The norm compliance dilemma (NCD) 3
2.2. Evolutionary dynamics 5
2.2.1. Homogeneous ODE model 5
2.2.2. Heterogeneous discrete-time model. 6
2.3. Network topologies 7
2.4. Simulation setup 7
3. RESULTS 8
3.1. Types of games - symmetric 2x2 games 8
3.2. Homogeneous infinite population. 9
3.2.1. Stability of fixed points 10
3.2.2. Phase plane visualizations 11
3.2.3. Area of basin of attraction 12
3.3. Well-mixed finite population 15
3.4. Networked populations 16
3.4.1. Random regular graph (RRG) 16
3.4.2. Random geometric graph (RGG) 17
3.4.3. The effect of the network topology 19
4. DISCUSSION 21
BIBLIOGRAPHY 23

1. INTRODUCTION

Evolutionary game theory has recently proven to be a powerful tool for understanding the complex behavioural mechanisms established between interacting rational agents. While in classical game theory such interactions are socially and temporally isolated, evolutionary game theory assumes an evolution over time: individuals can learn from other agents and imitate those adopting more successful strategies. In fact, it is thought that the extent of change in the strategy is determined by comparison with the aforementioned level of success: good behaviour is rewarded while bad is punished, in a form of survival of the fittest. Selection mechanisms in the natural world, such as human social systems, tend to work this way [1].

In this framework, in general, rational agents face a strategic decision between two options: cooperation and defection. A cooperator pays a cost to provide a benefit to all individuals with whom it interacts, whereas a defector does not bring any benefit, but receives those offered by neighboring cooperators. Indeed, defectors try to free ride from the efforts of the cooperating agents, but in doing so they threaten the success of the whole community [2]. Although competition between individuals should reward only selfish behavior, altruistic cooperation is observed in many contexts in nature. Five mechanisms have been proposed to describe the emergence and evolution of cooperation: kin selection, direct reciprocity, indirect reciprocity, network reciprocity, and group selection [3].

The difference between the benefits received and the cost spent determines the net gain or loss obtained by the agent in an interaction, and this value is referred to as the payoff. The most successful agents maximise their payoff and are therefore unlikely to change their strategy. In contrast, agents with a low payoff tend to improve it either by evaluating the payoffs associated with behavioral alternatives, i.e. best-response dynamics, or by copying the strategies that are more successful, i.e. replicator dynamics. In our study we adopted the latter. Both strategy update rules, however, are often implemented in theoretical models of human decision-making and are considered to be a standard assumption [4].

In our work, we use the framework of evolutionary game theory to model the decision-making process of individuals who face a potential epidemic outbreak. In these situations, individuals may take containment measures specific to the disease characteristics to avoid its spread. Most of them are spontaneous and rely on voluntary action, however, their adoption often results into a cost that is heterogeneously perceived by the population. Although this cost can often be interpreted as a mere economic expense, it must be also taken into account the time, energy and mental efforts consumed by the individual adopting the specific norm.

The "norm compliance dilemma" (NCD) we propose combines the framework of mathematical epidemiology with evolutionary game theory, with the aim of describing how and to what extent the presence of a disease influences human behaviour. Since we focus on behavioural mechanisms rather than the dynamics of epidemic spread, the model is intended to be general and applicable to a variety of situations. To cite a few examples, the disease under investigation could be COVID-19, and possible norms to prevent its spread include vaccination, wearing a mask, and hand disinfection [5]; or it could be a sexually transmitted disease, the prevention of which could consist of wearing a condom during sexual activity [6]; or also taking pre-exposure prophylaxis (PrEP) to prevent HIV [7]. For the sake of clarity, we will use the expression "comply with a norm" with the meaning of actively performing an action whose aim is to contain the spread of the disease.

To model the heterogeneous perceptions of individuals regarding the act of conforming to the chosen norm, we introduce the categories of "pro-norm" and "anti-norm" individuals. People

belonging to the first group are those who are willing to comply with the considered containment measure, or norm. Thus, the cost of adopting the norm for "pro-norms" individuals is considered to be negligible with respect to other costs involved in the game. On the contrary, those who are against such measure, or think it is not worth their effort to observe it, are defined as "anti-norm". It is important to emphasise that the willingness to comply with the measure does not automatically correspond to actual compliance, but rather describes the perceived effort in doing so, which is subjective and personal. This allows for the existence of individuals who adopt the measure despite being against it and individuals who do not adopt it despite being in favour of it, whether out of choice or obligation. The practical action of complying with the norm will be referred to as "cooperating", while refraining from adopting it will be "defecting"; whereas we will call "opinion" the agent's subjective effort in adopting the given norm.

Our aim is to investigate the evolution of cooperation and opinion over repeated iterations of the NCD game. Such evolution occurs since individual strategies are influenced by the behaviour of other agents. Similarly, opinions vary according to the present number of cooperators in the population. In infinite well-mixed populations, the strategy dynamics are usually described by the continuous-time replicator equations [8]. We firstly focused on this simplified population model, where the analysis was limited to symmetric situations, i.e., where agents perceive the same cost of compliance. Subsequently, while keeping the well-mixed structure, we analysed the effects of a finite population size, with a cost of compliance perceived heterogeneously among individuals, and a discretization of time. Finally, we moved towards a more experimental approach performing multi-agent simulations on networked populations, focusing on the structures of a random regular graph and a random geometric graph. The former was chosen to study the effect of low connectivity on a well-mixed population, and the latter to assess how the spatial arrangement of individuals affects the evolution of cooperation. Because analytic solutions were not possible in these cases, we adopted a numerical procedure, where time-evolution was treated as discrete.

2. METHODS

2.1. The norm compliance dilemma (NCD)

In our artificial population, agent i faces a strategic decision between cooperation ($s_i = 1$) or defection ($s_i = 0$). When it interacts with other agents, it receives a payoff that depends on its selected strategy s_i and on those of its neighbors s_j, where j are all agents interacting with i. Using the standard notation of evolutionary game theory [1], an interaction between two individuals choosing between cooperation and defection can be characterized by a 2×2 payoff matrix, where mutual cooperation leads to the reward R, mutual defection leads to the punishment P, while the mixed choice gives to the cooperator the sucker's payoff S and to the defector the temptation T. The values of the payoffs in the matrix are formed by the cost relative to the possibility of getting the disease and the cost of adopting the containment measure. While the former is fixed and equal for all individuals, the latter is purely subjective and varies according to the agents' opinion on the given norm. The "opinion" of agent i is measured by the variable $\alpha_i \in [0, 1]$, whose role is to tune the maximum cost of compliance to be paid when adopting the norm.

An agent who cooperates, i.e. complies with the norm, receives a discount in the probability of infection, but at the same time may pay a cost due to the adoption of that norm. If such agent is "anti-norm" ($\alpha_i = 0$), this cost will be maximum, while if it is "pro-norm" ($\alpha_i = 1$) it will be 0: cooperation towards the common cause of disease eradication for pro-norm agents outperforms the cost of adopting the norm. As a consequence, every agent in our model possesses a particular payoff matrix which depends on its opinion α_i. In the following table, we briefly introduce the relevant parameters of the model, which will be discussed in more detail later on.

$p_0 \in [0, 1]$	overall prevalence of the disease
$c_d = 1$	disease intrinsic cost
$c_n \in [0, 1]$	maximum cost of compliance to the norm
$\epsilon = 0.9$	disease cost discount for a cooperating agent
$\delta = 0.5$	disease cost discount when interacting with a cooperator

While here below we present a list of the variables:

$x \in [0, 1]$	fraction of cooperators
$\alpha \in [0, 1]$	population average opinion
$s_i \in \{0, 1\}$	strategy of agent i
$\alpha_i \in [0, 1]$	opinion of agent i

We show the payoff matrices of three different agents: a pro-norm agent (a), an anti-norm agent (b) and a generic agent with opinion α_i (c).

	C	D
C	$-p_0 c_d(1-\epsilon)(1-\delta)$	$-p_0 c_d(1-\epsilon)$
D	$-p_0 c_d(1-\delta)$	$-p_0 c_d$

(a) *Pro-norm payoff matrix*

	C	D
C	$-p_0 c_d(1-\epsilon)(1-\delta) - c_n$	$-p_0 c_d(1-\epsilon) - c_n$
D	$-p_0 c_d(1-\delta)$	$-p_0 c_d$

(b) *Anti-norm payoff matrix*

	C	D
C	$-p_0 c_d(1-\epsilon)(1-\delta) - c_n(1-\alpha_i)$	$-p_0 c_d(1-\epsilon) - c_n(1-\alpha_i)$
D	$-p_0 c_d(1-\delta)$	$-p_0 c_d$

(c) *Payoff matrix of agent i*

The first two are, of course, extreme cases of the latter, which are obtained by setting $\alpha_i = 1$ for the first and $\alpha_i = 0$ for the second. In Fig. 2.2 we illustrate a simple interaction between two agents, where the norm under study is the wearing of a face mask. In this example, the overall presence of the disease is set to $p_0 = 0.4$, the cost of compliance to $c_n = 0.5$, and the opinion of the agent i (on the left) to $\alpha_i = 0.5$. In this case, the most convenient choice is to adopt the opposite strategy of the other agent.

Figure 2.2
Illustration of a 2x2 game. The payoffs shown are relative to the agent i on the left, whose opinion is $\alpha_i = 0.5$. The parameters settings are: $c_d = 1$, $\epsilon = 0.9$, $\delta = 0.5$, $p_0 = 0.4$, $c_n = 0.5$.

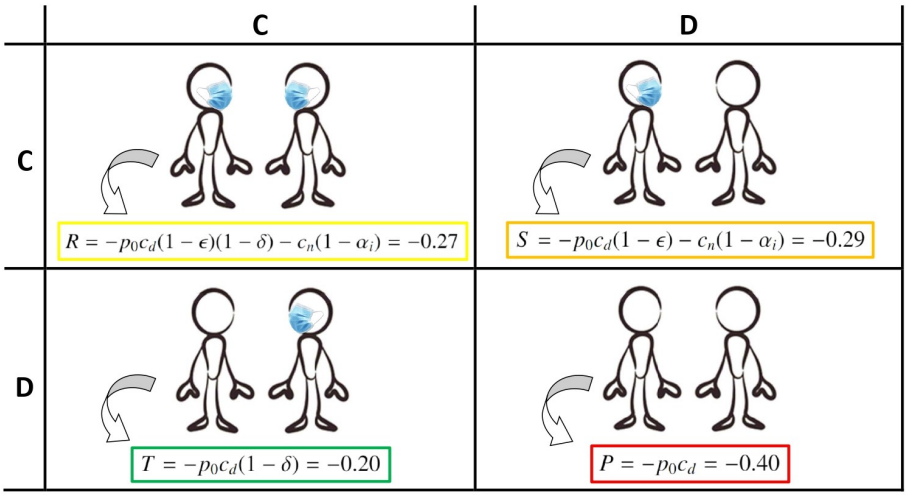

In the following, we discuss more in detail each of the aforementioned model parameters, and we justify the values that we set in our study.

- $\boldsymbol{p_0} \in [0, 1] \rightarrow$ the overall presence of the disease in the population.
  It spans from a fully susceptible population ($p_0 = 0$) to one where everyone is infected ($p_0 = 1$). Normally, it is a dynamical factor which changes during the process of the epidemic, but for simplicity we keep it fixed and we study settings with different values of p_0.

- $\boldsymbol{c_d} = 1 \rightarrow$ the disease intrinsic cost.
  It measures the cost to be paid by the individual who gets the disease, by taking into account its severity, the mortality, the availability of a therapy, and so on. In our study, we normalise this cost to 1, but it can be adjusted according to the characteristics of the disease under consideration.

- $\boldsymbol{c_n} \in [0, 1] \rightarrow$ the maximum cost of norm compliance.
  It is a factor that quantifies the effort required by the application of the containment measure. Depending on its value the agents will be more or less induced to cooperate. We set this parameter in the range [0, 1] because we are only interested in settings where c_n is positive and lower than the disease cost $c_d = 1$.

- $\boldsymbol{\epsilon} = 0.9 \rightarrow$ the disease cost discount for a cooperating agent.
  It measures the efficiency of the chosen containment measure and acts by reducing the probability of being infected, i.e. the cost of getting the disease. When $\epsilon = 0$ the adopted measure is completely useless, whereas when $\epsilon = 1$ the probability of contracting the disease for a cooperating agent drops to 0. However, both are extreme cases that do not reflect reality in

most situations: in our work we set $\epsilon = 0.9$ to study a particular containment measure which is efficient but not perfect in stopping inward transmission.

- $\boldsymbol{\delta} = 0.5 \rightarrow$ the disease cost discount for an agent that interacts with a cooperator.
  Since the adoption of the measure is often effective in stopping inward transmission as well as onward transmission, not only the cooperator itself benefits from its compliance, but also the agents with whom it interacts. The resulting reduction in the probability of being infected is measured by δ, which spans between 0 and 1. We set $\delta = 0.5$ in order to study a containment measure having higher efficiency in stopping inward rather than outward transmission, as for example in the case of a vaccine.

Two other important variables, cited in the aforementioned list but not yet discussed, are $x = \frac{1}{N}\sum_i s_i$, i.e. the fraction of cooperators in a population of N individuals, and $\alpha = \frac{1}{N}\sum_i \alpha_i$, i.e. the average opinion in the same population. The point $x = 1$ is reached when every agent in the population complies with the measure of containment ($s_i = 1, \forall i$), while $x = 0$ describes the opposite situation where no one does. On the other hand, when all the individuals are pro-norm ($\alpha_i = 1, \forall i$) the point $\alpha = 1$ is reached, while $\alpha = 0$ is obtained when all individuals are anti-norm.

2.2. Evolutionary dynamics

In our model, an agent can switch strategy by copying the one of an opponent, according to their respective payoffs. At the same time the agent may modify its opinion by being influenced by the strategies of other agents. When a given strategy is successful, i.e. it achieves higher payoffs with respect to the average payoff of the entire population, the fraction of individuals adopting it will increase in the next time step. In a similar manner, agents tune their opinion according to the present fraction of cooperators in the population. As a consequence, x and α evolve over time until the system reaches a steady state. One purpose of this work is to analyse the dynamics of the variables α and x, and to investigate how they behave under the effect of the parameters p_0 and c_n, as well the initial distributions of strategies and opinions.

2.2.1. Homogeneous ODE model

In this first part of the study we considered an infinite and well-mixed population, where everyone interacts equally likely with everyone else, and all players possess the same opinion $\alpha_i = \alpha$ (hence the term homogeneous). We remind that the fraction of cooperators x is given by the average of the individual strategies s_i in the population, while the fraction of defectors y is univocally determined by x, since $x + y = 1$. The evolution of strategies is governed by the replicator equations [8]:

$$\dot{x} = x(f_C - \bar{f})$$
$$\dot{y} = y(f_D - \bar{f})$$

where f_C and f_D are respectively the expected payoffs for cooperation and defection of the agents, while $\bar{f}$ is the average payoff of the entire population. Their explicit formulas read:

$$f_C = xR + (1-x)S = -p_0 c_d(1-\epsilon)(1-\delta x) - c_n(1-\alpha)$$
$$f_D = xT + (1-x)P = -p_0 c_d(1-\delta x)$$
$$\bar{f} = xf_C + yf_D = -p_0 c_d(1-\delta x)(1-\epsilon x) - xc_n(1-\alpha)$$

These equations assume that the probability of interacting with a cooperator is given by x, while with a defector by $y = 1 - x$. Since the dynamics of y is given automatically by knowing the one

of x, from now on we will only consider the latter. Simple calculations lead to the form:

$$\dot{x} = x(1-x)\Big[\epsilon p_0 c_d(1-\delta x) - c_n(1-\alpha)\Big] \tag{2.1}$$

A different procedure was adopted to describe the evolution of α, i.e. the average of the opinion α_i of each agent: it was created by introducing a factor $f(x, y)$ which denotes the feedback of strategists with the environment, the factors $\alpha(1-\alpha)$ to bound the evolution of α between 0 and 1, and the factor γ to tune the velocity of the variation of α. We adopted a simple linear feedback mechanism: $f(x, y) = x - y = 2x - 1$. The reason of this choice stems from the tendency of humans to follow the majority: when there are more people who cooperate, i.e. follow the norm, rather than those who defect, individuals tend to have a more favourable view of the norm itself. This being said, the formula of the α-update reads:

$$\dot{\alpha} = \gamma\alpha(1-\alpha)(2x-1) \tag{2.2}$$

Given this set of differential equations, the expected values of $x(t)$ and $\alpha(t)$ can be obtained by numerical integration, i.e. by discretising the continuous time to update the state variables $x(t)$ and $\alpha(t)$. The function we implemented works as follows: first, it calculates the instantaneous rates of change $\frac{dx}{dt}$ and $\frac{d\alpha}{dt}$ of our variables, then, it multiplies these derivatives by an appropriately small but finite time interval Δt, to yield an incremental change in the state variables. In formulas: $x(t+\Delta t) = x(t) + \Delta x$ and $\alpha(t+\Delta t) = \alpha(t) + \Delta\alpha$, where $\Delta x \approx \frac{dx}{dt}\Delta t$ and $\Delta\alpha \approx \frac{d\alpha}{dt}\Delta t$. Given the updated values, the process repeats.

2.2.2. Heterogeneous discrete-time model

In the second part of the study we considered a well-mixed but finite population of N individuals, each possessing a certain opinion $\alpha_i \in [0, 1]$ and a strategy $s_i \in \{0, 1\}$ (hence the term heterogeneous). In addition, to every agent corresponds a cumulative payoff Π_i^{cum} accumulated by performing the game with each neighbour and calculated as follows:

$$\Pi_i^{cum} = \sum_{j \in N_G(i)} \Pi(s_i, s_j) \tag{2.3}$$

where $N_G(i)$ denotes the set of neighbours of i, while $\Pi(s_i, s_j)$ is the payoff obtained by player i (with a certain α_i) adopting strategy s_i when playing against player j with strategy s_j. The evolution of strategies within this model is due to the fact that each agent adopts an imitation process in order to maximise its future payoff. In particular, the probability that agent i will change the strategy to the one of its neighbor j depends on the difference of the two cumulative payoffs $\Delta\Pi = \Pi_j^{cum} - \Pi_i^{cum}$, and is represented by the Fermi function:

$$P(s_i \leftarrow s_j) = \frac{1}{1 + e^{-\beta\Delta\Pi}} \tag{2.4}$$

Parameter β is the so-called intensity of selection: in the $\beta \to \infty$ limit, a player is always imposed the opponent's strategy when the former's payoff is lower than the latter's, but never otherwise. For $\beta \to 0$, however, worse-performing strategies may also be copied, as the decision-process becomes approximately random. In our study we set $\beta = 1$, which is a typical value broadly used in game theoretical models [9]. In order to describe the updating procedure for α, we introduce the variable x_i, i.e. the fraction of cooperation among the neighbours of i:

$$x_i = \frac{1}{N_i} \sum_{j \in N_G(i)} s_j \tag{2.5}$$

where N_i is the number of neighbours of agent i. Similarly to the infinitesimal incremental change of the continuous-time ODE model (see formula 2.2), the updated value of α_i is computed as:

$$\alpha_i^{new} = \alpha_i + \gamma\alpha_i(1 - \alpha_i)(2x_i - 1) \tag{2.6}$$

The role of parameter γ is to tune the speed of the change of variable α: the greater is γ the faster α adapts to the changes in x, that is to say, the opinion changes faster to adapt to individual strategies of the neighbours. In order to have similar behaviours for the time evolution obtained with the homogeneous ODE model, we set $\gamma = 1$.

2.3. Network topologies

We investigated two types of network structures: a random regular graph and a random geometric graph. A random regular graph (RRG) is a a particular kind of undirected random graph, which is constituted by a set of N nodes randomly connected with exactly k neighbours. In our graphs, the nodes correspond to the agents and the edges represent the connections between the agents, i.e. they connect the individuals exchanging the most significant interactions in terms of physical presence, with relative probability of infecting and being infected, but also in terms of opinion exchange. The simulations are performed on a population of $N = 300$ individuals where every agent, i.e. node, has exactly $k = 6$ neighbours and we assume the graph fixed for the duration of the evolutionary dynamics.

A random geometric graph (RGG) is a type of undirected graph often used to model social networks, given its spatial geometry that resembles the structures in which humans arrange themselves. This type of graph is constructed by randomly placing N nodes in some topological space, connecting two nodes by a link if their distance is less than a previously specified parameter $r \in (0, 1)$. Thus, the parameters r and N fully characterize a RGG. In our simulations we used the metric space $[0, 1]^2$ with the Euclidean distance, and the nodes were placed uniformly and independently in the underlying space. To compare the results obtained on the RRG we kept the same number of nodes $N = 300$ and we chose the radius of connectivity $r = 0.082$, in order to have an average number of neighbours $\bar{k} \approx 6$.

2.4. Simulation setup

We initialized the simulations assigning to each player i an initial strategy $s_i \in \{0, 1\}$, such that the fraction of cooperators x in the population was fixed, and an initial opinion α_i, taken from a uniform distribution with a fixed average α. Set the initial conditions, the simulation is performed over a sequence of steps. In each step we compute for every agent i the fraction of cooperators among its neighbours x_i (using formula 2.5) and its cumulative payoff Π_i^{cum} (using formula 2.3). While in the well-mixed population there was no need to calculate the fraction of cooperators for every node i (everyone sees the same $x_i \approx x$ corresponding to the cooperation fraction over the entire population), in the networks each agent can only see the fraction of cooperation x_i relative to its k neighbours, which has to be computed separately for all agents.

Then, we sequentially take each node in the network as player i and choose player j at random from i's neighbors. Agent i compares its own cumulative payoff with that of opponent j and has a chance to mimic its strategy, which is stored for later update. The update of the strategy occurs with probability given by formula 2.4, whereas the update of the opinion is given by formula 2.6. Once every agent has been taken and had the possibility to change its strategy and opinion, all the nodes in the graph simultaneously update their values of s_i and α_i, and the simulation proceeds to the next step .

3. RESULTS

3.1. Types of games - symmetric 2x2 games

The ranking of payoff elements determines the type of game being played. We introduce the two universal parameters [1] that are used to divide the games in their respective class: $D_g = T - R$ and $D_r = P - S$. When $D_g > 0$ and $D_r > 0$ the game is a Prisoner's Dilemma (abbreviated to PD), where players face a trade-off between the reach of a common good and a purely selfish interest. When $D_g > 0$ and $D_r \leq 0$ the game is a Snow Drift (SD), where players have an incentive to defect, but if they both do it, they pay a higher cost: the most convenient choice is to do the opposite of the other player. When $D_g \leq 0$ and $D_r > 0$ the game is a Stag Hunt (SH), while with $D_g \leq 0$ and $D_r \leq 0$ we are in a Harmony Game (HG), with no dilemma. In this initial part of the study, we consider a 2x2 game between individuals with homogeneous opinion $\alpha_i = \alpha$. We have:

$$D_g = -p_0 c_d \epsilon (1 - \delta) + c_n (1 - \alpha) \tag{3.1}$$

$$D_r = -p_0 c_d \epsilon + c_n (1 - \alpha) \tag{3.2}$$

According to the choice of the parameters p_0, c_n, and the opinion α, the game can vary between a PD, a SD and a HG: when $D_r = 0$, the game transitions between a PD and a SD game, whereas when $D_g = 0$, there is a transition between a SD and a HG. Accordingly, the game played is a SD when we have the following condition on c_n:

$$\frac{p_0 c_d \epsilon (1 - \delta)}{1 - \alpha} < c_n \leq \frac{p_0 c_d \epsilon}{1 - \alpha} \tag{3.3}$$

Figure 3.1
Types of game faced by a player with $\alpha = 0.5$. The black line is $c_n = \frac{p_0 c_d \epsilon}{1 - \alpha} = 1.8 p_0$, while the white one is $c_n = \frac{p_0 c_d \epsilon (1 - \delta)}{1 - \alpha} = 0.9 p_0$.

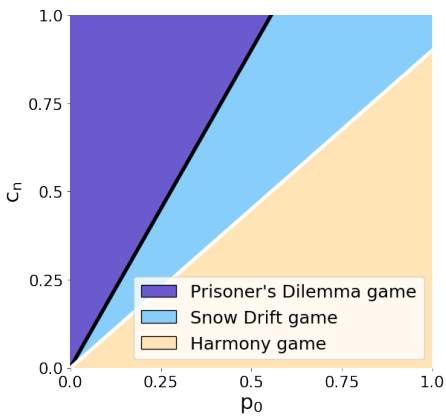

It is also interesting to discriminate the types of games according to the opinion α and the maximum cost of compliance c_n. The three following plots show the different areas related to each type of game: as expected, a greater area is related to a PD game when the overall presence of the disease p_0 is low, while as it increases, more combinations of α and c_n result in a HG, with no dilemma. In other words, when the prevalence of the disease is high, agents are more likely to comply with the norm: the discount offered by cooperation provides a higher payoff regardless of what other agents do.

Figure 3.2
The effect of the disease prevalence p_0 on the type of game.

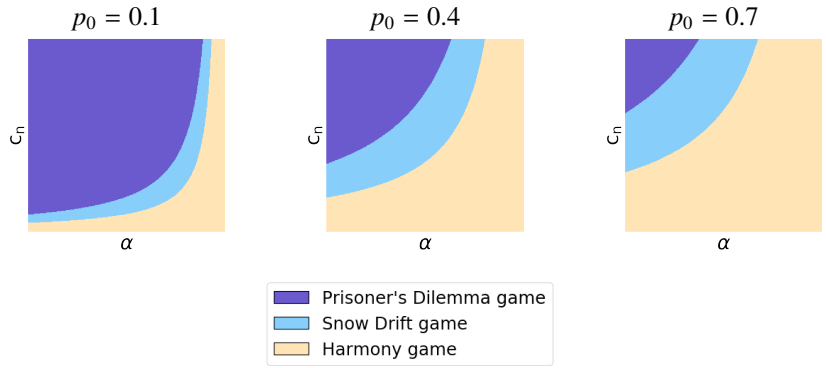

3.2. Homogeneous infinite population

In this section we present four relevant results obtained by numerically integrating the set of ordinary differential equations 2.1 - 2.2, as explained in section 2.2.1. The same examples will be repeated in the following sections, and the results compared.

Figure 3.3
Time evolution of $x(t)$ and $\alpha(t)$ within the continuous-time ODE model in a homogeneous infinite population. The initial average opinion $\alpha(0)$ is fixed to 0.25, while various values of $x(0)$ and of parameters p_0 and c_n are tested.

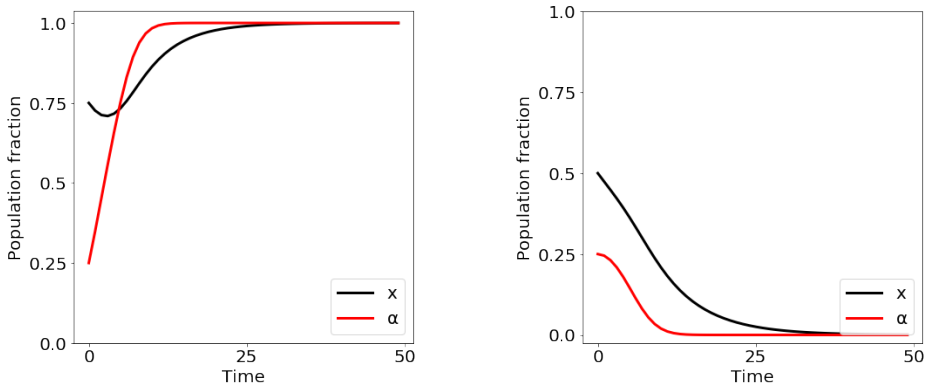

(a) $p_0 = 0.4$ *and* $c_n = 0.5$

(b) $p_0 = 0.4$ *and* $c_n = 0.5$

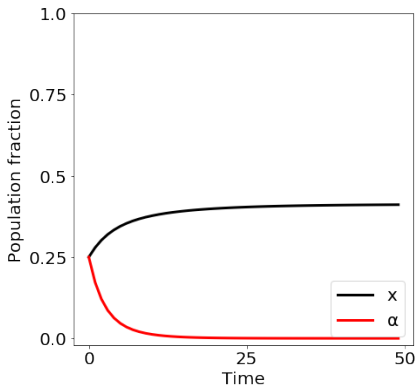

(c) $p_0 = 0.7$ *and* $c_n = 0.5$

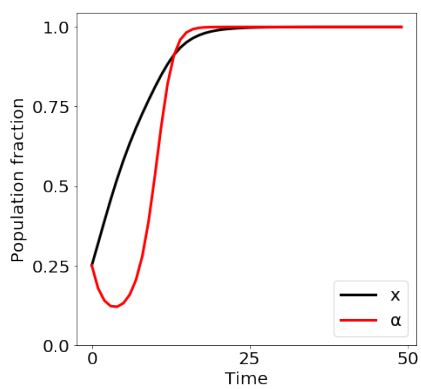

(d) $p_0 = 0.7$ *and* $c_n = 0.25$

As expected, the system evolves to the "pro-norm, fully cooperators" state when the initial condition $x(0)$ is high enough to allow α to rapidly increase and converge to 1 (Fig. 3.3a), or when the parameters describe a situation of high presence of the disease and low cost of compliance (Fig. 3.3d). Instead, for the cases where p_0 and c_n have comparable values, i.e. for the points in the p_0-c_n plane (relative to the present α) that correspond to a SD game, x may converge to a fixed value between 0 and 1: this is the case of Fig. 3.3c, where the convergence point is (0.41,0).

3.2.1. Stability of fixed points

The previous simulations converged to fixed values of x and α. These combinations of state variables represent stable points in phase space where the trajectories converge: they are among the so called "fixed points" of the system. The set of fixed points of the system:

$$\begin{cases} \dot{x} = x(1-x)\Big[\epsilon p_0 c_d(1-\delta x) - c_n(1-\alpha)\Big] \\ \dot{\alpha} = \gamma\alpha(1-\alpha)(2x-1) \end{cases} \tag{3.4}$$

is given by solving $\dot{x} = 0$, $\dot{\alpha} = 0$. We get the following six equilibrium solutions:

- $(x_1^*, \alpha_1^*) = (0, 0)$
- $(x_2^*, \alpha_2^*) = (0, 1)$
- $(x_3^*, \alpha_3^*) = (1, 0)$
- $(x_4^*, \alpha_4^*) = (1, 1)$
- $(x_5^*, \alpha_5^*) = \left(\frac{1}{2}, \frac{c_n - \epsilon p_0 c_d(1-\frac{\delta}{2})}{c_n}\right)$
- $(x_6^*, \alpha_6^*) = \left(\frac{\epsilon p_0 c_d - c_n}{\epsilon\delta p_0 c_d}, 0\right)$

The first four represent "boundary" fixed points, as they are found at the corners of our area of interest, formed by $[0, 1]^2$. The fifth fixed point is a "saddle point": a point that is stable for trajectories coming from two directions but unstable for all others. The condition for which this fixed point exists in the area of interest is given by:

$$c_n \geq p_0 c_d \epsilon\left(1 - \frac{\delta}{2}\right) \tag{3.6}$$

The sixth fixed point instead belongs to the x-axis, and again its existence in the area of interest depends on the choice of the model parameters. More precisely, it is found in the interval $x \in [0, 1]$ when:

$$\epsilon p_0 c_d(1-\delta) \leq c_n \leq \epsilon p_0 c_d \tag{3.7}$$

We note that this condition corresponds to the one for which we have a SD game given by eq. 3.3, in the case when $\alpha = 0$. We remark that we are analysing an infinite population of homogeneous opinion, where α represents the common opinion possessed by each agent. When $\alpha = 0$, i.e. all agents are anti-norm, the condition 3.7 implies that each player faces a SD game.

3.2.2. Phase plane visualizations

What happens when the system is not at one of the fixed points? There are several approaches to study the dynamics of the system: in our work we focused on two of them. The first one consists in analysing how the variables x and α change with respect to time, given some initial conditions $x(0)$ and $\alpha(0)$ and fixing the values of the parameters of the system. A second approach consists in analysing how each variable changes with respect to the other, with time being implicit rather than explicit. In this way, the dynamics of the coupled systems can be represented in terms of dynamics in phase space. In the phase portrait of Fig. 3.4, all possible initial conditions are simultaneously present in the same plane and the trajectories show the convergence point given each initial condition. In general, the dimensionality of the phase space is as large as the number of variables: in our case we have a $2D$ phase plane represented by $(x(t), \alpha(t))$.

In order to understand the trajectory in the phase space when far from the fixed point, it is useful to identify the so called "nullclines" of the system. A nullcline associated to a particular variable is the set of points in phase space for which its dynamical equation is set to 0. Thus, in our system we have x and α nullclines, respectively denoted by the green and red lines in the figure below. The intersections between the nullclines associated with x and α correspond to the fixed points found before.

Figure 3.4
Phase portrait of the ODE system (3.4) with $p_0 = 0.3$ and $c_n = 0.25$. Green lines are x nullclines, while red lines are α nullclines.

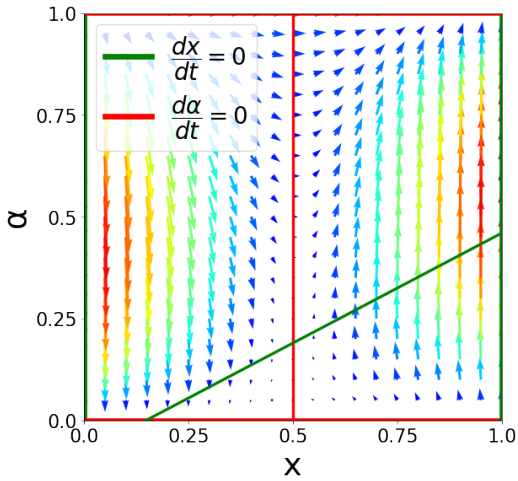

We analysed different scenarios according to the parameters p_0 and c_n. As it can be seen in Fig. 3.5, the effect of a high p_0 is to favour cooperation, while a high c_n tends to reduce it. In other words, agents cooperate more when there is a high prevalence of disease together with a low cost of compliance, as we would have expected. In addition, we note that if parameters p_0 and c_n are such that the game played on the x-axis is a HG, the system evolves towards the fixed point $(1, 1)$, despite of the initial conditions $x(0)$ and $\alpha(0)$ (see Fig. 3.5f). Instead, situations for which the game with $\alpha = 0$ is a SD (condition 3.7) result in the appearance of the fixed point on the x-axis (see Fig. 3.5c- 3.5e), which confirms what we found in the previous subsection.

Figure 3.5
The effect of p_0 and c_n on the evolution of cooperation and opinion.

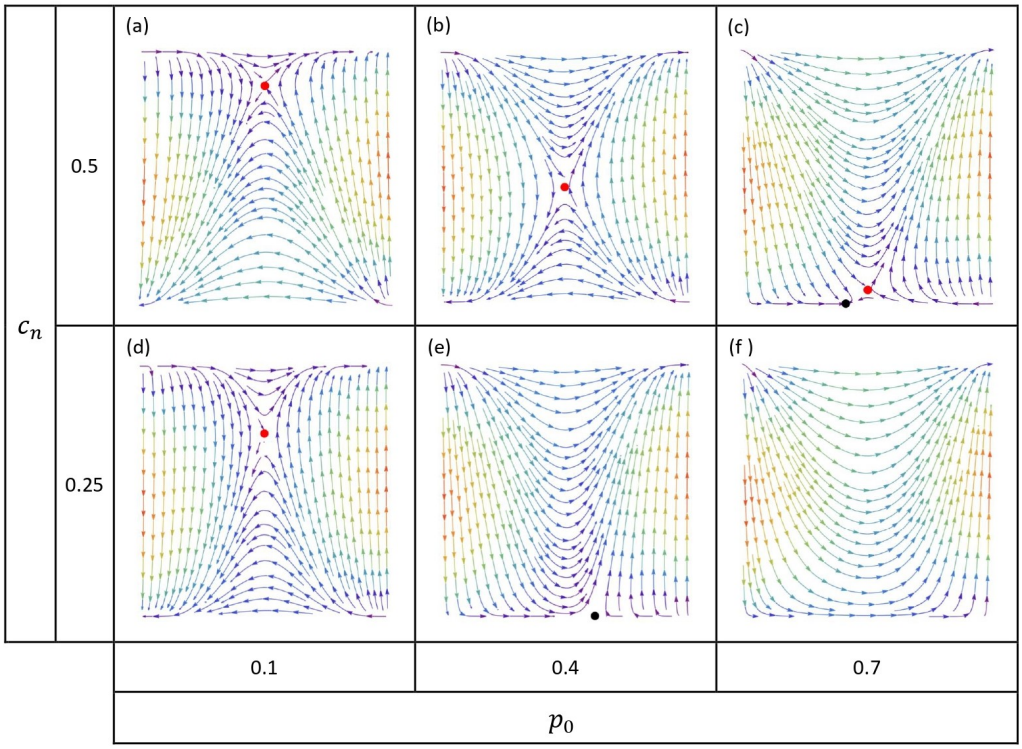

It is important to emphasise the following feature that is clearly visible in the phase space. When the average opinion is $\alpha = 1$, i.e. the entire population is pro-norm, the game played is always a HG, despite the choice of the parameters p_0 and c_n. In this case, there is no social dilemma and the system converges to (1,1). Instead, for $\alpha = 0$, we can have the three different games: a PD-type of game, where defection wins against cooperation and the trajectory converges to $(0, 0)$, a HG-type, where the trajectory converges to $(1, 1)$, and a SD-type, where the stationary solution is found inside the interval $x \in (0, 1)$ and its position depends on the parameters p_0 and c_n. We can therefore say that the HG found with $\alpha = 1$ couples with either a PD, a SD or with another HG with $\alpha = 0$.

3.2.3. Area of basin of attraction

We studied the final cooperation fraction averaged for all initial conditions in x and α, i.e. the mean value of $x(t)$ calculated for all trajectories in the phase space, after sufficient time t to guarantee convergence. From now on we will refer to this variable as "final cooperation", denoted with C_f. To do so, we numerically computed the basins of attraction of the fixed points using Mathematica. In particular, we computed the area $A_{1,1}$ of the phase plane composed by the trajectories converging to the stable stationary solution in $(1, 1)$, and the area $A_{x,0}$ of all trajectories converging to the fixed point on the x-axis, if present.

In the case of a coupling with a PD and a HG, we used the fixed point $(1, 1)$ as the attractor. In Fig. 3.6 we show two examples using the typical values for p_0 and c_n which we used in the previous subsection. We obtained respectively $A_{1,1} = 0.32$ and $A_{1,1} = 1$. In these cases, the final cooperation C_f corresponds to the value of the area $A_{1,1}$, since the only two stable points are in $x = 1$ and $x = 0$ and all trajectories converge to one of these two points.

Figure 3.6
Area of the basin of attraction of (1,1) computed numerically with Mathematica.

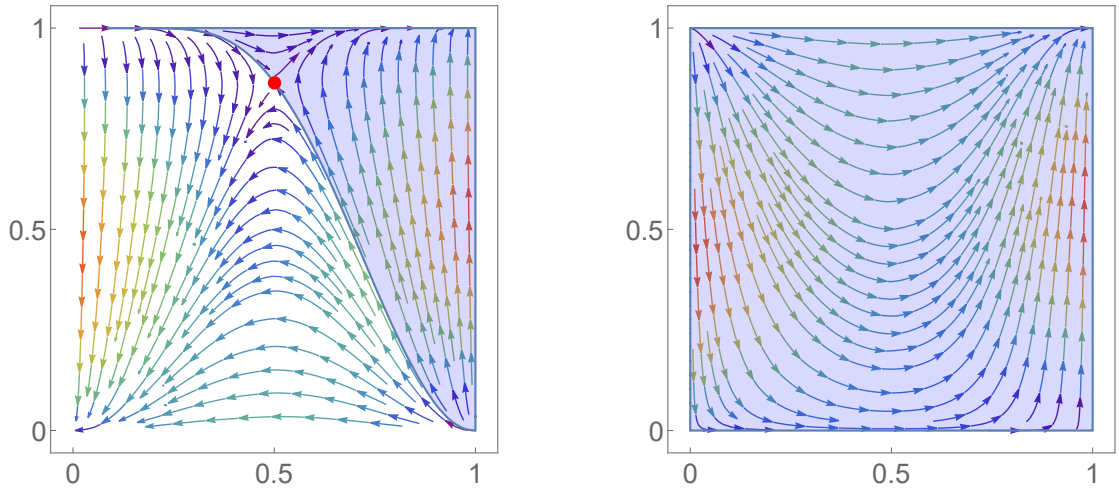

(a) *Coupling with a PD with* $p_0 = 0.1$ *and* $c_n = 0.5$

(b) *Coupling with a HG with* $p_0 = 0.7$ *and* $c_n = 0.25$

In the cases where condition 3.7 is satisfied, instead, we have a coupling with a SD game. Here, the final cooperation C_f does not simply correspond to the area $A_{1,1}$ as before, but instead is computed as:

$$C_f = \left(\frac{\epsilon p_0 c_d - c_n}{\epsilon \delta p_0 c_d}\right) A_{x,0} + (1 - A_{x,0}) \tag{3.8}$$

where $A_{x,0}$ is calculated dynamically towards the fixed point $(x_6^*, 0)$, with $x_6^* = \dfrac{\epsilon p_0 c_d - c_n}{\epsilon \delta p_0 c_d}$ that moves along the x-axis as the parameters are varied. In Fig. 3.7 we show the basin of attraction of the fixed point $(0.41, 0)$, having area $A_{x,0} = 0.24$, corresponding to a final cooperation fraction $C_f = 0.86$.

Figure 3.7
Area of basin of attraction of fixed point $(x_6^*, 0)$ *computed numerically with Mathematica.*

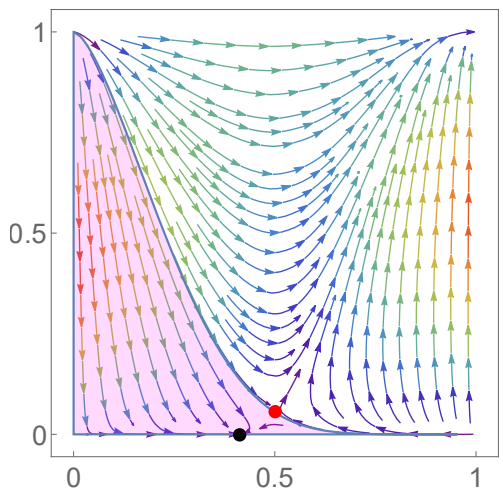

(a) *Coupling with a SD with* $p_0 = 0.7$ *and* $c_n = 0.5$

We computed the final cooperation fraction C_f for various values of p_0 and c_n, and we plotted the result in the heatmap below.

Figure 3.8
41x41 heatmap showing the final cooperation fraction for each combination of the parameters p_0 and c_n. The black and while lines delimit the types of games played on the x-axis, the orange line the fulfilment of the existence condition of the fixed point on the x-axis.

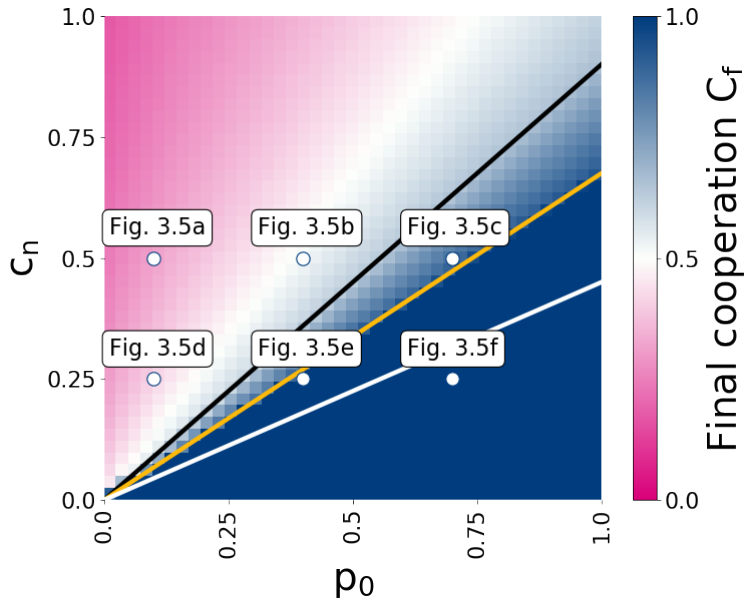

Similarly to Fig. 3.1, we have the coupling with the PD, SD or HG being separated by the black and the white lines. In particular, above the black line there is a coupling with a PD game, below the white line with a HG, and in between with a SD game. In Fig. 3.1, however, α was set to 0.5, while here is set to 0 as we are interested in distinguishing the types of games played on the x-axis. As evident in the heatmap, below the orange central line $c_n = \epsilon p_0 c_d(1 - \frac{\delta}{2})$ the final cooperation C_f is always 1: we are in the situations where all agents find more convenient to cooperate, and the average opinion converges to a fully pro-norm population. This is exactly what we would have expected below the white line $c_n = \epsilon p_0 c_d$, where there is a coupling with a HG, and no dilemma for any agent (Fig. 3.5f). Anyway, we see that the convergence towards $(1, 1)$ is also guaranteed in the slice of plane between the white and the orange line: we are here in settings where the fixed point on the x-axis exists and is found in $(0.5, 1]$, while the central saddle point does not exist (see condition 3.6). When this happens, although the coupling with a SD would suggest a lower cooperation fraction C_f, all trajectories converge to $(1, 1)$, as evident in Fig. 3.5e. The slice of plane inside the black and orange lines corresponds to situations where both the central saddle point and the fixed point on the x-axis are simultaneously present in the phase plane (see conditions 3.6 - 3.7 and Fig. 3.5c). As it can be seen, such region is darker than the one above the black line, due to the fact that here we are not only considering the area $A_{1,1}$ but we are also adding the contribution of the fixed point on the x-axis, as shown in formula 3.8. To conclude, the area above the black line concerns the couplings with a PD game: here the stable fixed points are found at $(0, 0)$ and $(1, 1)$, and all trajectories either converge to one or the other with a ratio that depends on the parameters p_0 and c_n (see Fig. 3.5a-3.5b-3.5d).

3.3. Well-mixed finite population

In this section we want to compare the results of the continuous ODE model with those obtained by simulating a well-mixed finite population within the heterogeneous discrete-time model (see section 2.2.2). As for the infinite well-mix population analysed above, agents interact with equal probability with all other agents. The difference is that in this case each individual i has its own strategy x_i and opinion α_i, which spans continuously between the extremes of pro-norm and anti-norm. To make the comparison clear, we show the same four examples presented in Fig. 3.3 in terms of the values of p_0, c_n, $x(0)$ and $\alpha(0)$, obtained by performing a simulation over 80 steps.

Figure 3.9
Time evolution of $x(t)$ and $\alpha(t)$ within the heterogeneous discrete-time model in a well-mixed population made of $N = 300$ individuals.

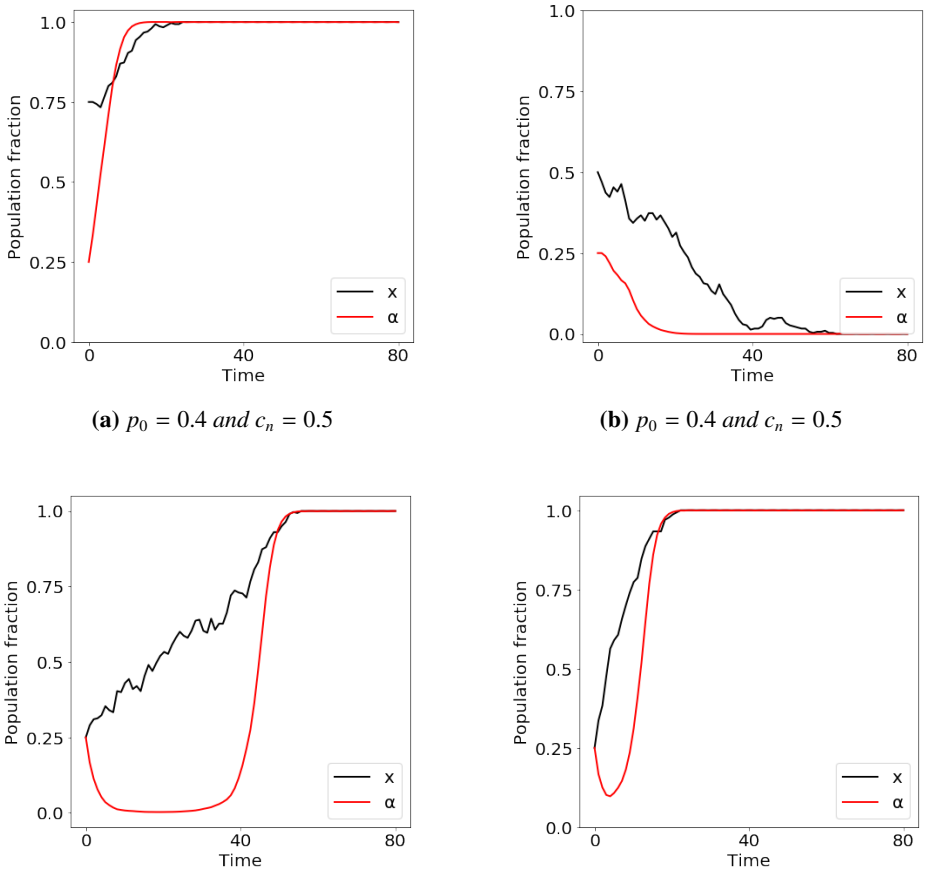

(a) $p_0 = 0.4$ *and* $c_n = 0.5$

(b) $p_0 = 0.4$ *and* $c_n = 0.5$

(c) $p_0 = 0.7$ *and* $c_n = 0.5$

(d) $p_0 = 0.7$ *and* $c_n = 0.25$

When the system is coupled with either a PD or a HG, the results obtained within the heterogeneous discrete-time model are reflecting those of the ODE model (see Fig. 3.9a - 3.9b - 3.9d compared with Fig. 3.3a - 3.3b - 3.3d). On the other hand, Fig. 3.9c is not in agreement with the corresponding Fig. 3.3c of the ODE model. Although we are starting the simulation at $(x(0), \alpha(0)) = (0.25, 0.25)$ and we have a coupling with a SD game, the system converges to $(1, 1)$, instead of $(0.41, 0)$ as Fig. 3.7 would suggest. This discrepancy is due to the finite-size effect on the system that makes the stochastic oscillations of x around the point 0.41 exceed $x = 0.5$. Consequently, variable α, which increases when $x > 0.5$, eventually converges to 1 and positively affects the increase in x.

3.4. Networked populations

So far, we have analysed a simplified model of an unstructured, well-mixed population in which everyone can interact with everyone else. This model can also be seen as a fully connected network, where individuals occupy the vertices of a graph and the edges determine who interacts with whom. However, real populations are not well-mixed: a more realistic scenario involves interactions not being random, but determined by spatial relationships or social networks [3]. In this part of the study, we aim at capturing the effect of the network structure on the evolutionary dynamics of the system. Furthermore, we investigate if and to what extent the evolution of cooperation is favoured by network structures.

3.4.1. Random regular graph (RRG)

We show here the same four simulations which were performed firstly within the continuous time ODE model and secondly on a well-mixed but finite population. To make the comparison clear, we kept the same population size $N = 300$ and we performed the simulations over a number of steps that ensures convergence. In this setting, the main difference with the previous models is that individuals, being spatially arranged on a RRG network, can only interact with a limited number of agents, i.e. with their $k = 6$ neighbours. What happens in the rest of the population is beyond the reach of the agent in question, who is therefore not affected by it in a direct way.

Figure 3.10
Time evolution of $x(t)$ and $\alpha(t)$ within the RRG model.

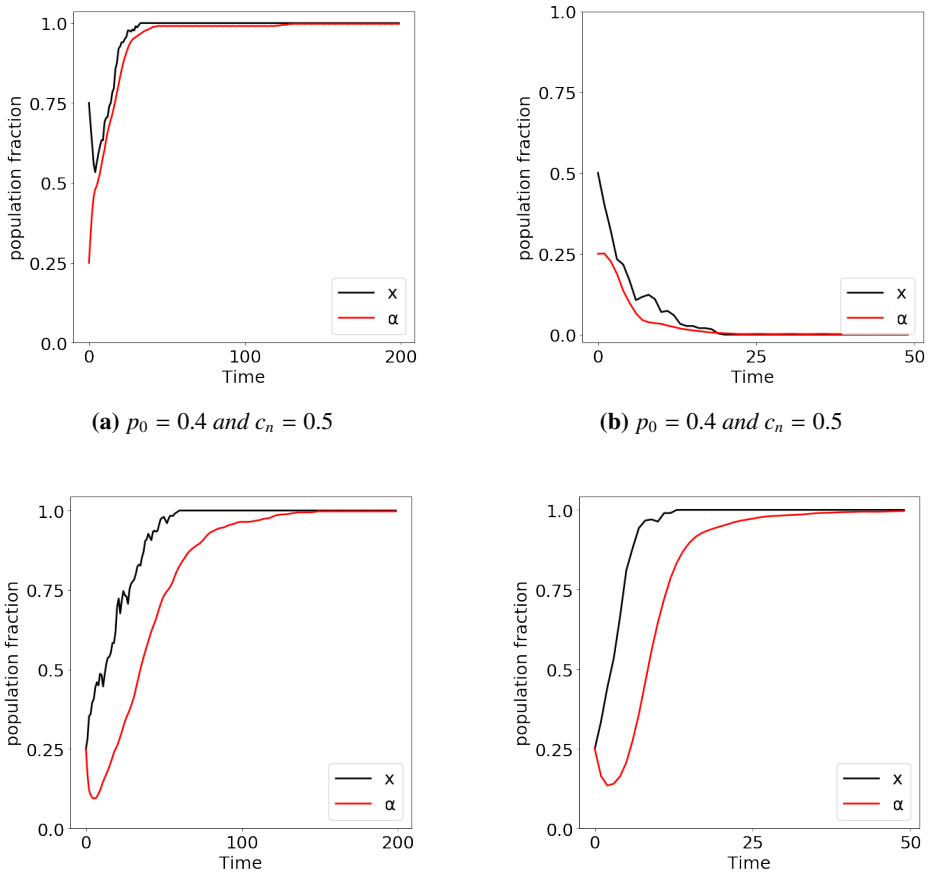

(a) $p_0 = 0.4$ *and* $c_n = 0.5$

(b) $p_0 = 0.4$ *and* $c_n = 0.5$

(c) $p_0 = 0.7$ *and* $c_n = 0.5$

(d) $p_0 = 0.7$ *and* $c_n = 0.25$

In general, we found that the simulations within this network structure are qualitatively similar to those of the well-mixed population, especially if k is increased. This was to be expected since the well-mixed population corresponds to a fully connected RRG, i.e. with $k = N - 1$. However, as evident in the simulations 3.10a- 3.10c performed over 200 steps, the network structure delays the convergence to the fixed point. This is due to the effect of the reduced number of neighbours, which makes a dominant strategy (or opinion) take longer to reach all nodes and impose itself on the population.

3.4.2. Random geometric graph (RGG)

As we did in the previous sections, we show the simulations performed with the same parameters, but this time in a population structure built with a RGG.

Figure 3.11
Time evolution of $x(t)$ and $\alpha(t)$ within the RGG model.

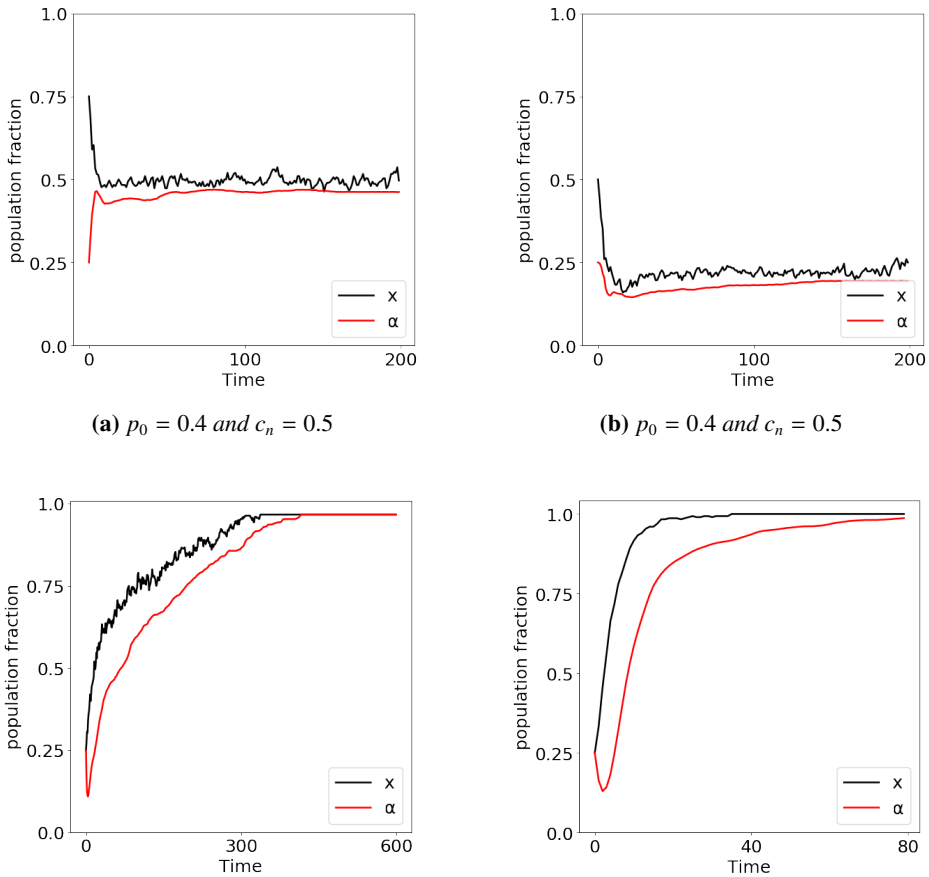

(a) $p_0 = 0.4$ *and* $c_n = 0.5$

(b) $p_0 = 0.4$ *and* $c_n = 0.5$

(c) $p_0 = 0.7$ *and* $c_n = 0.5$

(d) $p_0 = 0.7$ *and* $c_n = 0.25$

Interestingly, within this population structure the convergence towards fixed points $(1, 1)$ or $(0, 0)$ is delayed (see Fig. 3.11c - 3.11d), and in some cases it is not guaranteed (Fig. 3.11a - 3.11b). A similar delaying effect was also observed for the RRG, but here we see it amplified, as the RGG has a longer average path length [10], resulting in slower propagation of information (see Fig. 3.10c compared to Fig. 3.11c). In particular, RGGs are characterized by the presence of clusters, i.e. highly interconnected nodes in the population. Here, individuals share most interactions and copy one another, therefore they tend to conform to the same strategy (or opinion). It seems clear to us that the high clustering present in the RGG is at the root of the slow convergence to the fixed

points. For these reasons, the structure of RGGs seems appropriate to study the emergence and maintenance of cooperation in societies almost entirely made of defectors (and respectively the emergence of free-riders clusters in cooperative societies). To show this feature, we present in Fig. 3.12 an additional simulation, with the corresponding spatial arrangement of individuals.

Figure 3.12
Time evolution and final arrangement of cumulative payoffs, cooperation and opinion in a RGG of N=300 nodes and average number of neighbours $\bar{k} \approx 6$. *Setting:* $p_0 = 0.4$, $c_n = 0.5$, $x(0) = 0.5$, $\alpha(0) = 0.5$.

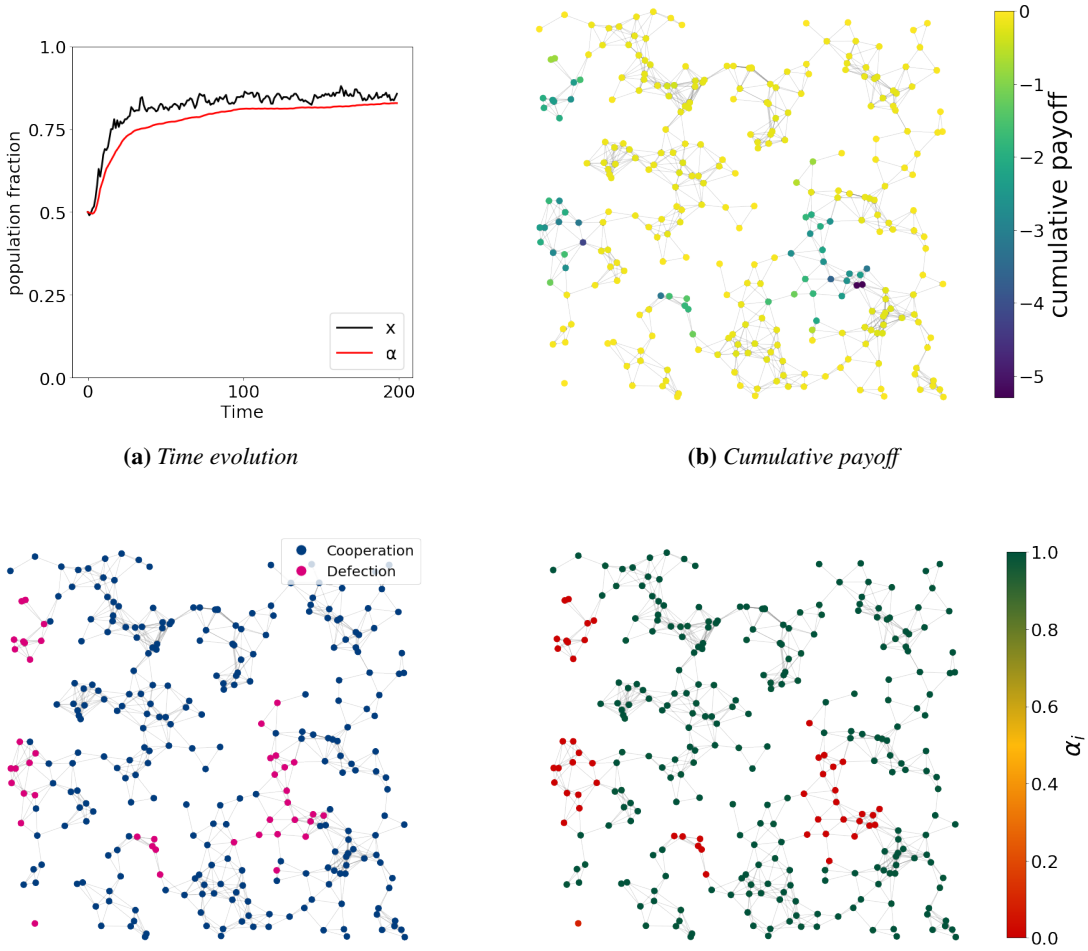

(a) *Time evolution*

(b) *Cumulative payoff*

(c) *Cooperation*

(d) *Opinion*

The simulation shows an initial increase in both variables, that then stabilise around a constant value. However, stochastic oscillations in the fraction of cooperators are observed. As mentioned above, the structure of the RGG may allow the assortment of cooperators (or defectors) in clusters that are more robust against invasion. In Fig. 3.12c we see the survival of clusters of defectors, even if they get a lower average payoff due to their higher probability of infection (see Fig. 3.12b). This is due to the process of imitation that is only carried out among neighbours. An agent surrounded by defectors is likely to become a defector, and at the same time its opinion α_i will decrease. Eventually, the system converges to situations where most cooperating agents are pro-norm, while defectors are anti-norm (see Figs. 3.12c and 3.12d). Most strategy updates occur at the borders: it's here that evolution takes place. Furthermore, it is common to see a mismatch between strategy and opinion at the borders. In Fig. 3.12b the two individuals that have the lowest payoff (in blue), are two anti-norm cooperators, who pay the full cost of compliance to the norm c_n.

Another interesting observation concerns the effect of the number of neighbours k, which is in average equal to 6, but can vary among the individuals. A cooperating agent pays a cost for all its k neighbours and receives a discount from each cooperator among them. However, since the payoffs are all negative and an agent's cumulative payoff is calculated over all its neighbours, the most favoured agents are actually those with the fewest neighbours (see the lonely individual in the lower left corner of Fig. 3.12b). It is interesting to make a comparison with the real world, where one of the measures to protect oneself from any contagious disease is to adopt social distance, since all interactions with other agents involve the possibility of contracting the disease. This aspect obviously could not be taken into account in the RRG, where each agent has a fixed number of neighbours.

3.4.3. The effect of the network topology

To give a visually clear impression of the effect of population structures on the evolution of opinion and cooperation, we present the following Fig. 3.13. We computed the final values of the average opinion α (first column) and the cooperation fraction x (second column) in the three population structures (well-mix in the first row, RRG in the second, RGG in the third). Each heatmap is a 21x21 matrix which shows the convergence value for each combination of p_0 and c_n. All simulations started from the initial conditions $(x(0), \alpha(0)) = (0.5, 0.5)$, they were performed over 300 steps ($t^* = 300$) and repeated 30 times to mitigate the effects of stochasticity.

We start by noting that the difference between the final average opinion $\alpha(t^*)$ and the cooperation fraction $x(t^*)$, in all three population structures, is negligible. This is in agreement with the previous results and confirms the fact that, in most cases and after sufficient time, $x(t)$ and $\alpha(t)$ evolve towards the same value. For this reason, in the next observations we will just refer to the cooperation fraction. For what concerns the well-mixed finite population and the RRG, the region of plane inside the two lines, or in its near proximity, results in a transition between an average of $x(t^*) = 1$ (in blue) and an average of $x(t^*) = 0$ (in magenta). We remind that these results are averaged twice: one is the average in the population $x(t^*) = \frac{1}{N}\sum_i s_i(t^*)$, and one is the average $\langle x(t^*)\rangle_s$ obtained over the 30 simulations. For these two population structures, the transitioning phase with $\langle x(t^*)\rangle_s \in (0, 1)$ is due to the average over the simulations. In fact, 300 steps are enough to ensure convergence and the system converges either to $x(t^*) = 1$ or to $x(t^*) = 0$, due to the stochastic oscillations of x (see Figs. 3.9 - 3.10). The smoother transition of the RGG shown in Fig. 3.13f, however, is not due to the average over simulations. In fact, in this case $x(t^*)$ does not necessarily converge to 1 or 0, but can, and most often does, acquire intermediate values (see Fig. 3.11).

Figure 3.13

Comparison of final average opinion and cooperation fraction for different population structures, starting from initial conditions $(x(0), \alpha(0)) = (0.5, 0.5)$. *The white lines delimit the area where both the central saddle point and the fixed point on the x-axis are simultaneously present in the phase plane* $(x(t), \alpha(t))$.

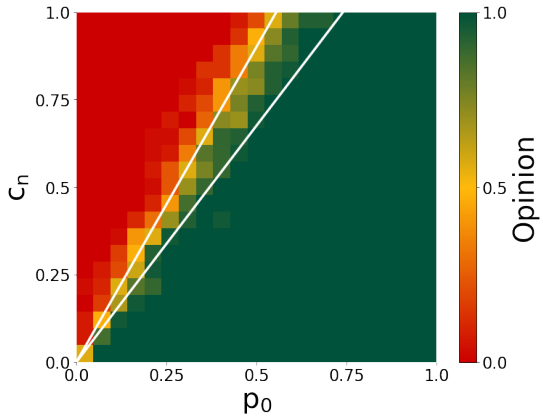

(a) *Well-mixed population - Average opinion*

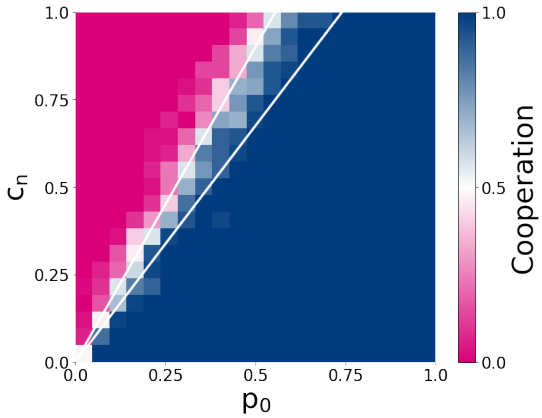

(b) *Well-mixed population - Cooperation fraction*

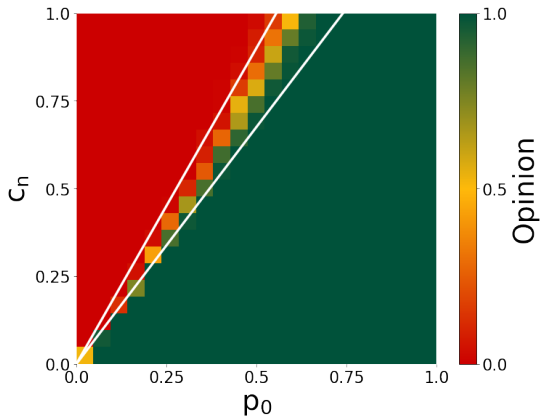

(c) *RRG Network - Average opinion*

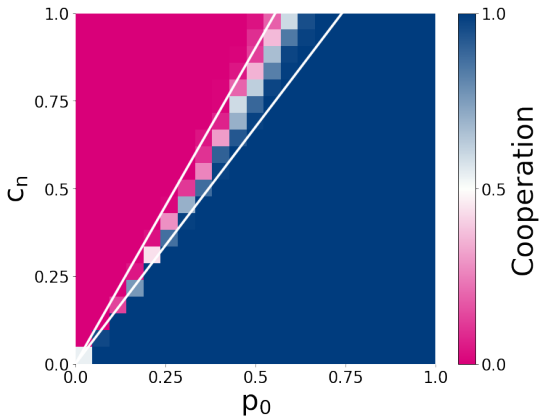

(d) *RRG Network - Cooperation fraction*

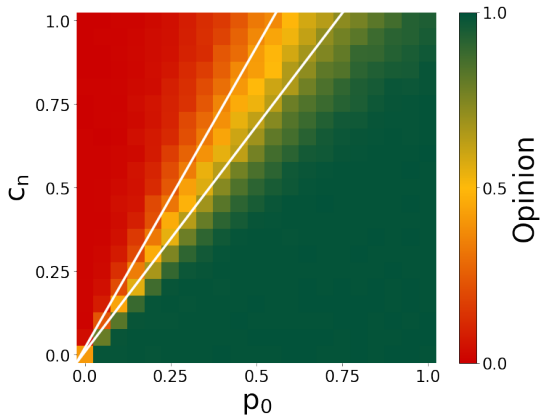

(e) *RGG Network - Average opinion*

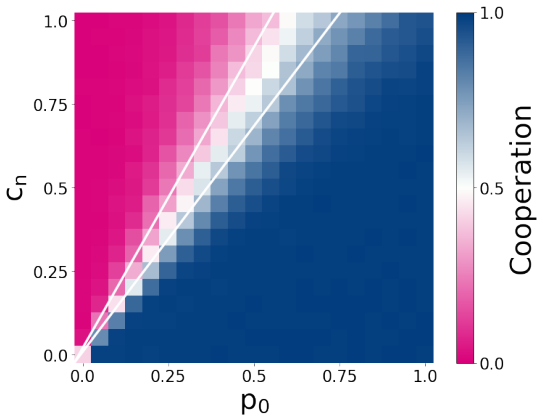

(f) *RGG Network - Cooperation fraction*

4. DISCUSSION

In many real societal systems, individuals experience distinct and very personal perceptions of the same interaction. This translates into the fact that payoffs do not depend solely on the strategies of the agents participating in a game, but also on their individualistic perception of the game itself. However, most models in evolutionary game theory assume homogeneous interactions both between agents and over time. Otherwise, in the case where they do consider heterogeneous payoffs, they primarily deal with interactions between two distinct populations, e.g. two-species biological systems [11], or in which individuals possess different roles, e.g. the Battle of the Sexes [12]. In our work, we investigated the effect of distinct, time-evolving perceptions of interactions. In particular, we focused on how this perception, which we called "opinion", propagates and evolves in different population structures. In our model, this opinion corresponds to the agent's individual effort in "adopting the norm", i.e. actively taking an action to contain the spread of the disease. We referred to a "cooperator" as one who respects the norm, while one who does the opposite was called a "defector".

Our norm compliance dilemma (NCD) represents a new framework which involves evolution of cooperation together with opinion dynamics. It is intended to be general and applicable to different coevolutionary games. In fact, the results we obtained are specific to the values of the cost of getting the disease, c_d, and the inward and outward efficiency of the containment measure, ϵ and δ respectively. Other choices of the aforementioned parameters correspond to different real-world scenarios, e.g. a higher value of disease cost could be set to model a more severe disease, along with lower values of inward and outward efficiency to describe a less effective containment measure, or norm. We firstly constructed a differential equation model which was solved analytically for an infinite population of homogeneous perception; then, we compared the results with those obtained in finite populations having heterogeneous individual perceptions and arranged in network structures.

One of the purposes of this study was to investigate the impact of the two parameters we kept free: the presence of the disease in the population, p_0, and the maximum cost of compliance to the norm, c_n. We found that a high presence of the disease favours cooperation and causes the preponderant opinion in the population to be in favour of the norm, or "pro-norm". On the contrary, a high cost of compliance results in less cooperation and a higher presence of "anti-norm" individuals. This result holds qualitatively for all population structures, regardless of spatial arrangement or heterogeneity of opinions. A possible implementation of our model could be to let p_0 change dynamically as the number of cooperators changes in time. This could be done by coupling our evolutionary decision-making model to a disease-spreading model, as suggested by the Vaccination Dilemma [13].

Another purpose of the study was to assess the effect of the population structure on the evolution of cooperation. Previous works have shown that certain network structures promote cooperative behaviour, especially if they have a low connectivity [14]. According to our results, we could evince that spatial arrangement of individuals is responsible for the survival of cooperation communities in a society almost entirely made of defectors. Symmetrically, defection communities arise and endure in cooperative societies. It is interesting to note how this reflects reality: people who exchange relevant interactions reinforce each other's opinions and often end up acting in the same way. For this reason, spatial networks have once again proven to be a powerful tool for shaping real-life social interactions.

The large variability of the final cumulative payoffs of individuals in spatial structures inspires the idea of implementing an adaptive network, i.e. a network that changes its structure, evolving in

time. In terms of our model, individuals facing a potential epidemic outbreak could decide to adopt social distancing by removing the connections they have with some individuals. This corresponds to change their number of neighbours k, which would become a new dynamical variable of the model, together with x and α. For example, an agent with few neighbours interacting with an agent with many neighbours might decide to sever the connection with the latter, fearing the cost of the disease.

Another possible extension of the model consists in the introduction of a multiplex network [15]. In this structure, each type of interaction between nodes takes place on a separate network layer. In our case, it would be useful to build two distinct layers: a "contact network" and an "opinion dynamics network". The first one would describe the face-to-face interactions within which the disease can spread, e.g. people on a bus, co-workers sharing the same office, family, neighbours, friends. The second one, instead, would concern the connections where opinions propagate, e.g. through social networks, phone calls, meetings.

BIBLIOGRAPHY

1. Ito, H. & Tanimoto, J. Scaling the phase-planes of social dilemma strengths shows game-class changes in the five rules governing the evolution of cooperation. *Royal Society open science* **5,** 181085. ISSN: 2054-5703. https://europepmc.org/articles/PMC6227953 (Oct. 2018).
2. Antonioni, A., Martinez-Vaquero, L. A., Mathis, C., Peel, L. & Stella, M. Individual perception dynamics in drunk games. *Phys. Rev. E* **99,** 052311. https://link.aps.org/doi/10.1103/PhysRevE.99.052311 (5 2019).
3. Nowak, M. A. Five Rules for the Evolution of Cooperation. *Science* **314,** 1560–1563. eprint: https://www.science.org/doi/pdf/10.1126/science.1133755. https://www.science.org/doi/abs/10.1126/science.1133755 (2006).
4. Laland, K. Social Learning Strategies. *Learning & behavior* **32,** 4–14 (Mar. 2004).
5. Pradhan, D., Biswasroy, P., Kumar Naik, P., Ghosh, G. & Rath, G. A Review of Current Interventions for COVID-19 Prevention. *Archives of Medical Research* **51,** 363–374. ISSN: 0188-4409. https://www.sciencedirect.com/science/article/pii/S0188440920306159 (2020).
6. Zenilman, J. M. *et al.* Condom Use to Prevent Incident STDs: The Validity of Self-Reported Condom Use. *Sexually Transmitted Diseases* **22,** 15–21. ISSN: 01485717, 15374521. http://www.jstor.org/stable/44964674 (2022) (1995).
7. Okwundu, C., Uthman, O. & Okoromah, C. Antiretroviral pre-exposure prophylaxis (PrEP) for preventing HIV in high-risk individuals. *Cochrane database of systematic reviews (Online)* **7,** CD007189 (July 2012).
8. Nowak, M. A. in *Evolutionary Dynamics: Exploring the Equations of Life* 45–70 (Harvard University Press, 2006). ISBN: 9780674023383. http://www.jstor.org/stable/j.ctvjghw98.7 (2022).
9. Roca, C. P., Cuesta, J. A. & Sánchez, A. Evolutionary game theory: Temporal and spatial effects beyond replicator dynamics. *Physics of Life Reviews* **6,** 208–249. ISSN: 1571-0645. https://www.sciencedirect.com/science/article/pii/S1571064509000256 (2009).
10. Melnik, S. & Gleeson, J. Simple and accurate analytical calculation of shortest path lengths (Apr. 2016).
11. Cressman, R. Evolutionary Game Theory with Two Groups of Individuals. *Games and Economic Behavior* **11,** 237–253. ISSN: 0899-8256. https://www.sciencedirect.com/science/article/pii/S0899825685710500 (1995).
12. Rapoport, A. & of Michigan Press, U. *Two-person Game Theory: The Essential Ideas* ISBN: 9780472050154. https://books.google.es/books?id=d9hQAAAAMAAJ (University of Michigan Press, 1966).
13. Kabir, K. M. A., Jusup, M. & Tanimoto, J. Behavioral incentives in a vaccination-dilemma setting with optional treatment. *Phys. Rev. E* **100,** 062402. https://link.aps.org/doi/10.1103/PhysRevE.100.062402 (6 2019).
14. Fehl, K., van der Post, D. & Semmann, D. Co-evolution of behaviour and social network structure promotes human cooperation. *Ecology letters* **14,** 546–51 (Apr. 2011).
15. De Domenico, M. *et al.* Mathematical formulation of multilayer networks. *Physical Review X* **3,** 041022 (2013).